IL NUOVO CIMENTO Vol. 36 C, N. 5 Settembre-Ottobre 2013
DOI 10.1393/ncc/i2013-11591-5

Colloquia: QCDN12

Recent results on PHENIX longitudinal asymmetry measurements

I. Nakagawa for the PHENIX Collaboration

RIKEN - 2-1 Hirosawa, Wako, Saitama 351-0198, Japan
RIKEN BNL Research Center, Brookhaven National Laboratory - Upton, NY 11973, USA

ricevuto il 18 Aprile 2013

Summary. — The spin structure of proton has been a long-standing open question for the last decades. Polarized DIS and SIDIS experiments have been the explorer of the field and providing us the knowledge the part of substructure of the proton spin by its subcomponents. In contrast to well-measured valence quark contribution to the proton spin, polarization of gluons and sea quarks still remain with a large uncertainty. PHENIX experiment has been providing various asymmetry data to introduce new constraints to the proton spin structure, particularly gluon and sea quark polarization in proton spin using the world highest-energy polarized proton-proton collider, RHIC. In this report, the latest gluon polarization measurements in PHENIX through various observables are presented. Also preliminary results of W-boson production to measure the sea quark polarization in both central and forward rapidity are presented.

PACS 13.88.+e – Polarization in interactions and scattering.
PACS 13.38.Be – Decays of W bosons.
PACS 13.85.Qk – Inclusive production with identified leptons, photons, or other nonhadronic particles.
PACS 14.20.Dh – Protons and neutrons.

1. – Introduction

Helicity parton density functions (PDFs) carry vital information on the extent to which quarks and gluons with a given momentum fraction x have their spins aligned with the spin direction of a fast-moving nucleon in a helicity eigenstate. Recent QCD analyses model various functional forms for PDFs [1] and attempt to decompose the contribution from each subcomponent partons, *e.g.* quarks and gluons to the total proton spin through the global fitting to available polarized deep inelastic scattering (DIS) and semi-inclusive DIS experiments [2]. The attempt has been quite successful to constrain the quark spin contribution to be only $\sim 30\%$, while contributions from the gluon, sea quark spin, and the orbital angular momenta of quarks and gluon have remained

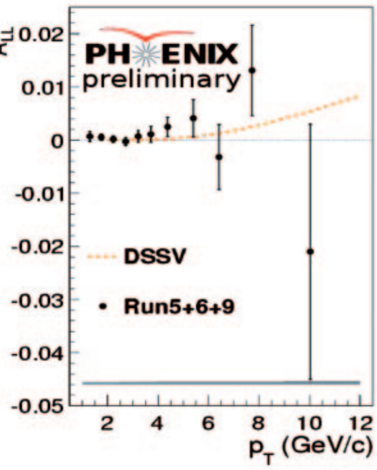

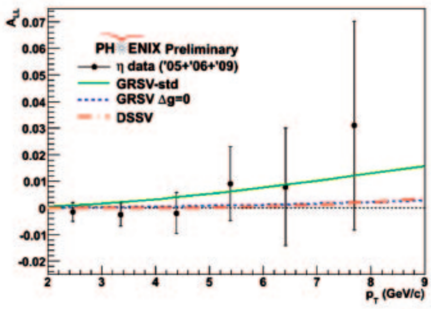

Fig. 1. – Longitudinal double spin asymmetry for π^0 (left) plotted and η (right) as a function of P_{T}.

uncertain. The gluons, which make up roughly 50% of the total (unpolarized) partonic momentum distribution, may be expected to carry a significant fraction of the nucleon spin, but this distribution could previously only be determined by scaling violations in inclusive DIS over the limited range in Q^2 of available data [2]. The world highest polarized proton-proton collider, RHIC provide the powerful and unique approach to some of these poorly known subcomponents of proton spin with good precision. Under the parturbative QCD regime, direct access to gluons is possible through parton-parton scattering. Not only for gluon polarization ΔG, it also introduces the new generation measurements of sea quark polarization through parity violation asymmetry of W-boson production, taking the full advantage of the high-energy-polarized-proton beam.

2. – Polarized gluon distribution

Through run 9, PHENIX has recorded a total of approximately $25\,\mathrm{pb}^{-1}$ (summed over run 5, run 6, and run 9) of longitudinally polarized $p+p$ collisions at 200 GeV. The double- helicity asymmetry in neutral pion production has been the flagship measurement by PHENIX sensitive to ΔG, given the abundance of pions and the excellent PHENIX capability to trigger on the π^0 decay to two photons. The cross-section is dominated by partonic quark-gluon scattering for $p_{\mathrm{T}} > 5\,\mathrm{GeV}/c$, so the process is directly sensitive to gluon. π^0 yields are estimated from the invariant mass spectrum reconstructed from two photon pairs observed in central arm electromagnetic calorimeters. Backgrounds are estimated using sidebands around the π^0 mass peak. A_{LL} measurements of neutral pion production at $\sqrt{s} = 200\,\mathrm{GeV}$ are compared with one of global QCD fit model predictions [1] in fig. 1, left panel. Data are combined for run 5, 6 and 9. Statistical precision is getting improved as run goes by, providing tight constraint on the gluon polarization in region $0.02 < x < 0.2$. On the other hand, the systematic error (gray band) starts to dominate the total uncertainty in low P_{T} region. The primary source of the systematic error comes from relative luminosity monitoring between positive and negative bunches, whose precision is required to the level of $\sim 10^{-4}$. The impact of π^0 data to the gluon polarization on global QCD fits based on the DSSV framework has been studied in reference [3] in conjunction with recent preliminary jet A_{LL} results from STAR.

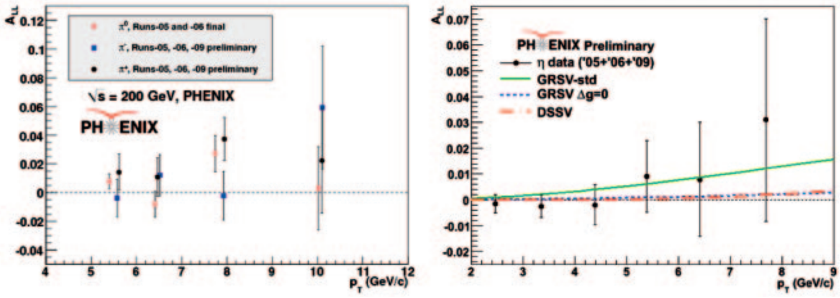

Fig. 2. – A_{LL} (left) for charged pions plotted as a function of P_{T}. A_{LL} for clusters observed by MPC plotted as a function of P_{T} (right). Solid band represents the size of systematic uncertainty.

As the available luminosity has increased, in particular with the 2009 data set, other probes have become increasingly interesting. Preliminary results for A_{LL} in η meson production at gluon polarizations (shown in fig. 1 right panel) were made possible by the recent parametrization of the η fragmentation functions for the first time, including PHENIX η cross section data from 2003 and 2006 in addition to world e^+e data.

A_{LL} measurement of charged pions serves unique sensitivity to the sign of ΔG in conjunction of π^0 data by the ordering of the three pion species asymmetries, *i.e.* $A_{\mathrm{LL}}^{\pi^+} > A_{\mathrm{LL}}^{\pi^0} > A_{\mathrm{LL}}^{\pi^-}$ if Δg is positive [4]. Shown in fig. 2 left panel is A_{LL} data of charged pions for run 5, run 6, and run 9 combined in compared with π^0 A_{LL}. Unfortunately statistics for charged pions are rather limited compared to copious π^0 data because the charged pions are not as well measured as π^0 since PHENIX lacks a dedicated charged hadron trigger. Statistical accuracy will be further improved by the ongoing long and high statistics run-13 experiment, which is executed with longitudinally polarized proton beams at $\sqrt{s} = 510\,\mathrm{GeV}$.

Even though the measurements have become very precise and have started to constrain the gluon polarization, all available data are limited kinematic range, namely relatively large x region. Observation in limited kinematic range naturally raises a question, such as what is the gluon polarization at low x where the gluon density in the proton is largest, and can higher-twist contributions become important while the leading twist contribution is small? In order to answer the question, it is very important to extend the x-range of the PHENIX measurements and provide information on the x dependence of ΔG. Even if the gluon polarization falls off with decreasing x, the integral ΔG is dominated by contributions from $x < 0.1$ since this is the region where the gluons are most abundant. It is thus important to measure ΔG to values of x as far below 0.1 as feasible. PHENIX has attempt to measure the gluon polarization in forward rapidity by utilizing the Muon Piston Calorimeter (MPC) $3.3 < \eta < 3.7$ to measure the inclusive cluster A_{LL}. According to a Monte Carlo simulation, the cluster is dominated by π^0 whose fraction is predicted to be $70 \sim 80\%$ depends on P_{T} bin. Rests are contribution from direct photons, η, charged hadrons and others. The kinematic range now extends the gluon sensitivity to an order of magnitude lower x, as low as level of $\sim 10^{-3}$. Preliminary results are plotted in fig. 2 right panel as a function of cluster's P_{T}. One may notice that the cluster measurement in forward rapidity region again faces to serious precision competition between statistics and systematic error which is represented by black bar in the figure. The dominant cause of the systematic error is the relative luminosity as same scenario as π^0 case. The improvement of the relative luminosity measurement has already been implemented before run 13 in order to reduce the systematic uncertainty.

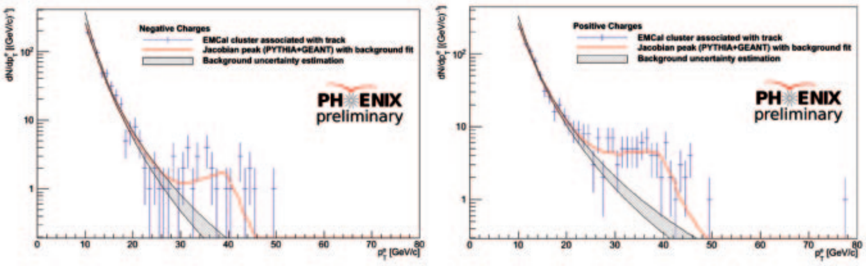

Fig. 3. – (Left) Single muon P_{T} distributions before (green) and after tight event selection cuts optimized for W-boson extraction for MuID (red) and high momentum trigger samples (green), respectively. Shown in open histograms are data and solid histograms are breakdown of contributed spectra of hadron fake high P_{T} (purple), heavy flavor decay (cyan) backgrounds and W and Z boson signals (red). (Right) Longitudinal Single spin asymmetries plotted as a function of rapidity. Data are compared with various global QCD fit predictions. Both graphs show for South (top) and North (bottom) results.

3. – Polarized sea quark distribution

The production of $W^{\pm}$ bosons at $\sqrt{s} = 500\,\mathrm{GeV}$ provides an ideal tool to study the spin-flavor structure of sea quarks inside the proton. The left-handed W boson only couples to (anti)quarks of a certain helicity, giving rise to large parity-violating single spin asymmetries A_{L} in longitudinally polarized $p + p$ collisions at RHIC. In addition, the coupling of the W's to the weak charge correlates directly to quark flavor. $W^{\pm}$-boson productions are simplified to be described by $u + d$ $(d + u)$ interactions, ignoring quark mixing. RHIC is complementary to semi-inclusive DIS measurements in that the distributions are probed at a much higher scale ($M_W^2 = 6400\,\mathrm{GeV}^2$). Here in PHENIX, the W boson was detected through its leptonic decay mode, *i.e.* single electron in central and muon in forward arms. Therefore, the measurement of sea quark polarization via W-boson production is clean and direct observation because no fragmentation function is involved in this process. The observed A_{L} for W^+ and W^- can be described as linear combination of contributions from polarized valence and sea quarks:

$$(1)\quad A_{\mathrm{L}}^{W^+} = \frac{\Delta u(x_1)\bar{d}(x_2) - \Delta\bar{d}(x_1)u(x_2)}{u(x_1)\bar{d}(x_2) + \bar{d}(x_1)u(x_2)}, \qquad A_{\mathrm{L}}^{W^-} = \frac{\Delta d(x_1)\bar{u}(x_2) - \Delta\bar{u}(x_1)d(x_2)}{d(x_1)\bar{u}(x_2) + \bar{u}(x_1)d(x_2)}.$$

Shown in fig. 3 is P_{T} distribution of single electrons (left) and positrons (right) candidates observed in central arm rapidity region $\eta < 0.35$ from electromagnetic calorimeter and RICH trigger (ERT) event samples. The experimental spectrum was fitted with P_{T} shape of $W^{-(+)} \to e^{-(+)}$ events predicted by PYTHIA and the power row counting curve to mimic background yield. The power row counting curve was determined in low P_{T} region where background process dominates the yield. The estimated background fraction in the signal region $50 > P_{\mathrm{T}} > 30\,\mathrm{GeV}/c$ was 14–17%.

The observed longitudinal single spin asymmetries for W^+ and W^- from so extracted W yields are plotted in fig. 4 left and right panel, respectively. Data points represent run-9 result [5] (red), and Run11 (blue), respectively and they are consistent within statistical error. These data are compared with global fit predictions drawn as a function of rapidity. The combined results of run-9 + run-11 data (black) show well improved statistical precision. Data are still consistent with selected model predictions compared here within 1 sigma.

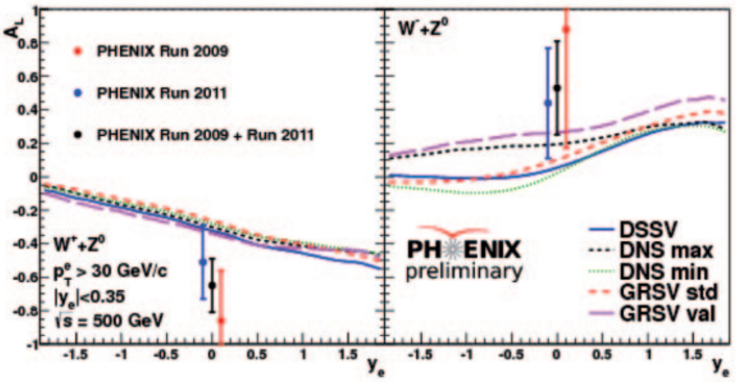

Fig. 4. – Longitudinal single spin asymmetry for W^+ (left) and W^- (right) plotted as a function of rapidity.

On the other hand, model predictions diverge in larger positive (negative) rapidity region for $W^{+(-)}$-boson production compared to these of central rapidity region. The divergence is primarily driven by our present poor knowledge about sea quark polarization. Due to unbalanced parton x_1 and x_2 combination, the contribution to $A_L^{W^{+(-)}}$ from $\Delta\bar{d}$ $(\Delta\bar{u})$ polarization term can be enhanced in eq. (1). While sensitivity to sea quark polarization is enhanced in forward rapidity region, the measurement becomes

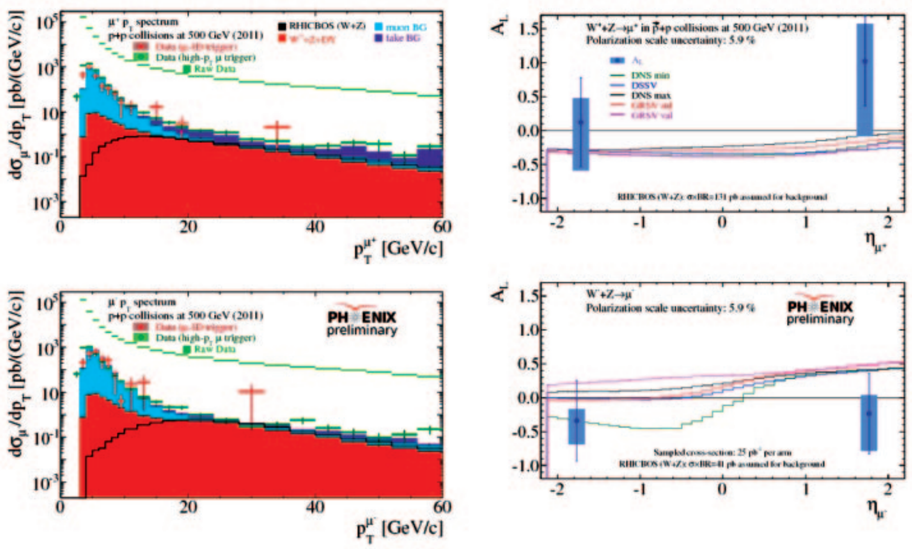

Fig. 5. – (Left) Single muon P_T distributions before (green) and after tight event selection cuts optimized for W-boson extraction for MuID (red) and high momentum trigger samples (green), respectively. Shown in open histograms are data and solid histograms are breakdown of contributed spectra of hadron fake high P_T (purple), heavy flavor decay (cyan) backgrounds and W and Z boson signals (red). (Right) Longitudinal Single spin asymmetries plotted as a function of rapidity. Data are compared with various global QCD fit predictions. Both graphs show for South (top) and North (bottom) results.

more challenging compared to that in central rapidity region. Shown in fig. 5 left panels are P_{T} distributions of single μ^+ (top) and μ^- (bottom) candidates in forward rapidity region. In addition to raw spectra, experimental data after tight event selection cuts are presented by open histograms. The decomposition of contributing sub-processes (signal W/Z, hadron, and heavy flavor decay single muon backgrounds) are superimposed by solid histograms in the same graph. Unlike small contamination of backgrounds in the signal W region for central arm, background contribution still does not die out even in very high $P_{\mathrm{T}} > 30\,\mathrm{GeV}/c$ region for the forward muon case. The estimated S/N ratio is about 1/3 as of the preliminary phase. This is primarily due to the degraded momentum resolution as higher the momentum, which is the intrinsic characteristics of momentum measurement by a magnetic spectrometer in contrast to the energy measurement by the electromagnetic calorimeters in central arm. However, there is still room to improve the S/N ratio by improving the momentum resolution of the muon tracker (MuTr), which yet hasn't been demonstrated designed performance. Efforts to improve its performance have been in progress in both hardware/software wise.

Shown in right panels of fig. 5 are the first measurements of A_{L} W^+ (top) and W^- (bottom) in forward/backward rapidity, respectively. Although statistical errors are large, the measurements are executed in the region where different theoretical models varies in their predictions. We are to take about a factor of 10 more statistics by run 13 to improve the statistical precision.

REFERENCES

[1] de Florian D., Sassot R., Stratmann M. and Vogelsang W., *Phys. Rev. Lett.*, **101** (2008) 07200; *Phys. Rev. D*, **80** (2009) 034030.

[2] COMPASS Collaboration, *Phys. Lett. B*, **690** (2010) 466; *Phys. Lett. B*, **693** (2010) 227, references therein.

[3] Aschenauer E. C. *et al.*, *The RHIC Spin Program: Achievements and Future Opportunities*, nucl-ex/arXiv:1304.0079.

[4] Kawall D. for PHENIX Collaboration, *J. Phys.: Conf. Ser.*, **230** (2010) 012040.

[5] Adare A. *et al.*, *Phys. Rev. Lett.*, **106** (2011) 062001.